An Ink Spreading Model for Dot-On-Dot Spectral Prediction

Roger David Hersch, Adish Kumar Singla
School for Computer and Communication Sciences,
Ecole Polytechnique Fédérale de Lausanne (EPFL), Switzerland

Abstract

Due to increasing printing accuracies and the possibility of printing several droplets at the same pixel location, there is a renewed interest in dot-on-dot printing models. In the present contribution, we improve a dot-on-dot spectral prediction model relying on the Yule-Nielsen modified Spectral Neugebauer model by taking into account ink spreading in all ink superposition conditions. Since ink spreading is different when ink dots are printed alone, printed in superposition with one ink or printed in superposition with two inks, we create for each superposition condition an ink spreading function mapping nominal to effective dot surface coverages. When predicting the reflection spectrum of a dot-on-dot halftone patch, its known nominal surface coverage values are converted into effective coverage values by weighting the contributions from different ink spreading functions according to the corresponding ratio of colorant surface coverages. We analyze the colorimetric prediction improvement brought by our ink spreading model for dot-on-dot thermal transfer prints and for ink-jet prints. Accounting for ink spreading according to different ink superposition conditions considerably improves the prediction accuracy. In the case of ink jet prints at 120 lpi, the mean $\Delta E94$ difference between predictions and measurements is reduced from 4.54 to 1.55 (accuracy improvement factor: 3). Due to the slight misregistration between the ink layers, spectral predictions accounting for ink spreading in the case of dot-on-dot screens are less accurate than corresponding predictions for classical mutually rotated screens.

Keywords*: Color printing, color halftone, dot-on-dot printing, spectral prediction model, Yule-Nielsen effect, spectral Neugebauer model, dot gain, ink spreading, ink superposition conditions, effective surface coverages, tone reproduction curves.*

Introduction

Many different phenomena influence the reflection spectrum of a color halftone patch printed on a diffusely reflecting substrate (e.g. paper). These phenomena comprise the surface (Fresnel) reflection at the interface between the air and the paper, light scattering and reflection within the substrate (i.e. the paper bulk), and the internal (Fresnel) reflections at the interface between the paper and the air. The lateral scattering of light within the paper substrate and the internal reflections at the interface between the paper and the air are responsible for what is generally called the optical dot gain, known as the *Yule-Nielsen* effect.

In addition, due to the printing process, the deposited ink dot surface coverage is generally larger than the nominal coverage, yielding a "mechanical" dot gain (hereinafter called "ink spreading"). Effective ink dot surface coverages depend on the inks, on the paper, and also on the specific superpositions of an ink halftone and the other inks.

At the present time, according to the literature [1][2], among the existing spectral reflection prediction models, mainly the well-known Yule-Nielsen modified spectral Neugebauer model [3][4] is used for predicting reflection spectra.

There has been a renewed interest in dot-on-dot printing, since high accuracy printing devices are available and since recent ink-jet devices may incorporate, besides the classical cyan, magenta, yellow and black inks, additional custom inks such as light magenta, light cyan, red, orange, green and dark blue. Printing with more than 3 inks with classical mutually rotated screens may induce undesirable moiré effects [5]. Precise dot-on-dot printing may therefore be a solution for moiré-free printing with more than three custom inks. However, dot-on-dot printing requires precise registration of the color layers in order to avoid color shifts [6].

A variant of the Yule-Nielsen modified Spectral Neugebauer (YNSN) model has been proposed for dot-on-dot printing [7][2]. This dot-on-dot model is limited to single ink surface optimization. It does not consider the fact that the amount of ink spreading (also known as "mechanical" dot gain) strongly depends on which other ink(s) an ink halftone is superposed.

In the present contribution, we develop a dot-on-dot spectral prediction model accounting for ink spreading in the different superposition conditions. The new dot-on-dot spectral prediction model includes the equations for computing colorant surface coverages (also called "Neugebauer primaries") from ink surface coverages. Since ink spreading is different when dots are printed alone, printed in superposition with one ink or printed in superposition with two inks, we create ink spreading functions which map nominal to effective surface coverages in every specific superposition condition. This is carried out by fitting effective dot surface coverages which minimize the sum of square differences between the measured reflection density spectra and reflection density spectra predicted according to the spectral dot-on-dot Yule-Nielsen modified Neugebauer model.

For the prediction of color halftone reflection spectra, nominal surface coverages of a halftone are converted into effective surface coverages by weighting the contributions from different ink spreading functions according to the ratio of colorant surfaces contributing to that halftone.

In order to optimize the n-value of the spectral Yule-Nielsen modified Neugebauer model for a given printer and a screen frequency, we compute, for a subset of halftone samples, the mean CIELAB $\Delta\Delta E_{94}$ color difference between predicted and measured reflection spectra. By iterating across possible n-values, we select the n-value yielding the lowest mean color difference.

The benefit of the new dot surface coverage model is verified by comparing measured color halftone patch reflection spectra and predicted reflection spectra for 729 patches produced by generating all combinations of inks at nominal coverages of 0%,

13%, 25%, 38%, 50%, 63%, 75%, 88% and 100%. The CIE-94 $\Delta\Delta E_{94}$ color difference formula gives a measure of the visually perceived distance between measured and predicted spectra.

The measurements are carried out with a Gretag Eye-One photospectrometer having a $45^o/0^o$ geometry.

The dot-on-dot Yule-Nielsen modified spectral Neugebauer model

In early prediction models of color halftone prints, the term "dot gain" encompasses both the physical dot gain (the enlargement of the printed dot) and the optical dot gain due to the lateral propagation of light. The spectral Neugebauer model [9][4] predicts the reflection spectrum of a color halftone patch as the sum of the reflection spectra of its individual colorants (Neugebauer primaries) weighted by their fractional area coverages a_i.

$$R(\lambda) = \sum_i a_i \cdot R_i(\lambda) \tag{1}$$

In dot-on-dot screens [2], each dot is exactly printed in superposition with the other dots (Figure 1). The colorants that are present within a given superposition of cyan, magenta and yellow dots depend on their respective surface coverages. For example, in Figure 1, with an ink dot surface relationship $c <= m <= y$, the corresponding area coverages of the colorants black (superposition of cyan, magenta and yellow), red (superposition of yellow and magenta), yellow (yellow printed alone) and white are the following:

$$\begin{aligned} a_k &= c && \text{; surface coverage of colorant black} \\ a_r &= m\text{-}c && \text{; surface coverage of colorant red} \\ a_y &= y\text{-}m && \text{; surface coverage of colorant yellow} \\ a_w &= 1\text{-}y && \text{; surface coverage of colorant white} \end{aligned} \tag{2}$$

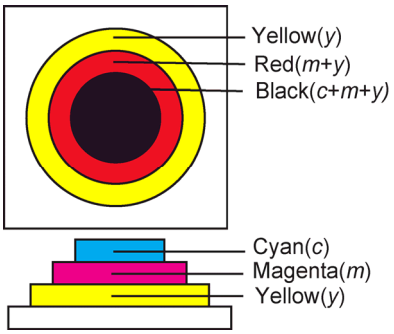

Figure. 1. *Graphical representation of dot-on-dot printed cyan, magenta and yellow dots, for the case c <= m <= y*

Equivalent equations for the colorant coverages can be established for the other ink dot size relationships (Table 1).

Table 1. Colorant area coverage equations for each of the 6 possible ink dot surface relationships

Area Cover-ages	*c≤m≤y*	*c≤y<m*	*m<c≤y*	*m≤y<c*	*y<c≤m*	*y<m<c*
a_w	*(1–y)*	*(1–m)*	*(1–y)*	*(1–c)*	*(1–m)*	*(1–c)*
a_c	*0*	*0*	*0*	*(c–y)*	*0*	*(c–m)*
a_m	*0*	*(m–y)*	*0*	*0*	*(m–c)*	*0*
a_y	*(y–m)*	*0*	*(y–c)*	*0*	*0*	*0*
a_r	*(m–c)*	*(y–c)*	*0*	*0*	*0*	*0*
a_g	*0*	*0*	*(c–m)*	*(y–m)*	*0*	*0*
a_b	*0*	*0*	*0*	*0*	*(c–y)*	*(m–y)*
a_k	*c*	*c*	*m*	*m*	*y*	*y*

Since the spectral Neugebauer model neither takes explicitly into account the lateral propagation of light within the paper bulk nor the internal reflections (Fresnel reflections) at the paper-air interface, its predictions are not accurate [10]. Yule and Nielsen [3] modeled the non-linear relationship between the reflection spectra of paper and solid ink and the reflection spectra of single ink halftones by a power function, whose exponent n is fitted according to a limited set of measured halftone patch reflection spectra. Viggiano [4] applied the Yule-Nielsen relationship to the spectral Neugebauer equations, yielding the *Yule-Nielsen modified Spectral Neugebauer model* (YNSN):

$$R(\lambda) = \left(\sum_i a_i \cdot R_i(\lambda)^{\frac{1}{n}} \right)^n \tag{3}$$

This YNSN model is often used for the characterization of printing systems [2][11][12][16][13]. Yule and Nielsen [3] have shown that when light scattering within the paper bulk has no effect, e.g. when the light scattering distance is much smaller than the screen element period, the n-factor is 1. In the case of full scattering, i.e. when the light scattering distance is important in respect to the screen element period, we have n=2. However, as underlined by Yule and Nielsen and later by Rogers [18], larger n factors may occur since, due to the Fresnel reflection at the interface between the print and the air, a large part of the light emerging from the paper bulk and reaching the print-air interface is reflected back into the paper bulk [19]. In the case of ink-jet printers, n-factors as large as n=10 are reached [15], probably due to the presence of many different ink thickness levels within the printed dots .

Dot surface coverages accounting for ink spreading

Ink spreading is present when an ink halftone is printed in superposition with another solid ink or when an ink halftone is printed in superposition with two or more solid inks. In a similar manner as the physical dot gain of a single ink halftone patch printed on paper, ink spreading tends to enlarge the effective surface of a printed dot and tends to lower the resulting reflection spectrum, i.e. it yields slightly darker colors. Figure 2 shows examples of dot gain, defined as the effective dot surface coverage minus the nominal dot surface coverage, for an ink halftone printed alone on paper and printed in superposition with the other

solid inks, in the case of dot-on-dot magenta ink-jet prints at 75 lpi (Figure 2a) and of dot-on-dot thermal transfer prints at 75 lpi (Figure 2b).

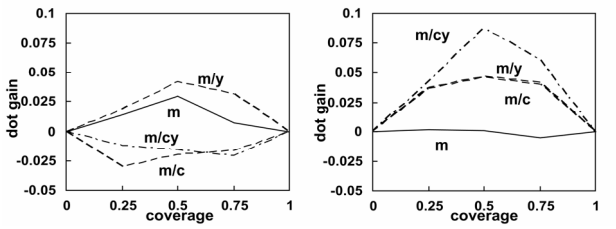

(a) Inkjet: (b) Thermal transfer:

Figure. 2*. Dot gain as a function of nominal coverages, for ink halftones at 75 lpi, printed alone (solid line) and in superposition with other solid inks (dotted lines), (a) for an ink-jet print and (b) for a thermal transfer print.*

In respect to dot-on-dot printing, Balasubramanian [7] computed effective dot surface coverages by considering only the dot gain of single ink halftones printed on paper. Xia, Saber, Sharma and Tekalp [17] also assumed for each ink halftone a single mapping between nominal and effective surface coverages. They obtained this mapping by performing a total least square regression relative to single ink halftones and to multi-ink gray halftones. Other attempts to model ink spreading were restricted to classical mutually rotated screens [12][15] or to spectral prediction models accounting for variable ink density [14].

Ink spreading model

We compute the effective surface coverages in ink layer superpositions by relying on the assumption that when a halftone ink layer is printed *either beneath or on top* of a solid ink layer, its effective surface coverage is modified. Separate ink spreading functions establish the mapping of nominal surface coverages to (a) effective surface coverages of single ink halftones, (b) effective surface coverages of single ink halftones superposed with one solid ink and (c) effective surface coverages of single ink halftones superposed with two solid inks. In order to obtain the effective coverages (c', m', y') of the inks of a color halftone patch as a function of the nominal coverages (c, m, y), we weight the contributions of the different surface coverage functions according to their corresponding relative colorant surfaces.

During the calibration of the model, the functions mapping nominal to effective surface coverages of single ink halftones printed on paper white, on one solid ink or on two solid inks are obtained by fitting effective surface coverages (e.g. at 25%, 50% and 75% nominal coverages) of an ink using the spectral prediction model given by equation (3). We obtain for each nominal surface coverage an effective (fitted) surface coverage. By linear interpolation between the so obtained effective surface coverages, we obtain the ink spreading functions (similar to tone reproduction curves) mapping nominal to effective surface coverages of each ink halftone in each ink superposition condition.

Let us consider the 3 cyan, magenta and yellow inks with nominal surface coverages c, m and y. The ink spreading functions mapping nominal to effective surface coverages for single ink halftones printed on paper are $f_c(c)$, $f_m(m)$ and $f_y(y)$. The ink spreading functions mapping nominal to effective ink surface coverages, for single ink halftones superposed with a second solid ink and for single ink halftones superposed with two solid inks are:

$f_{c/m}(c)$: *cyan* of coverage c superposed with solid ink *magenta*;
$f_{c/y}(c)$: *cyan* of coverage c superposed with solid ink *yellow*;
$f_{m/c}(m)$: *magenta* of coverage m superposed with solid ink *cyan*;
$f_{m/y}(m)$: *magenta* of coverage m superposed with solid *yellow*;
$y_{y/c}(y)$: *yellow* of coverage y superposed with solid ink *cyan*;
$y_{y/m}(y)$: *yellow* of coverage y superposed with solid *magenta*;
$f_{c/my}(c)$: *cyan* of coverage c superposed with solid *magenta* and *yellow*;
$f_{m/cy}(m)$: *magenta* of coverage m superposed with solid *cyan* and *yellow*;
$f_{y/cm}(y)$: *yellow* of coverage y superposed with solid *cyan* and *magenta*.

In the case of three inks, these 12 functions may for example be obtained by fitting 36 patches, i.e. 3 patches (25%, 50% and 75% nominal coverages) per function.

Figures 2a and 2b give examples of dot gains (effective surface coverage minus nominal surface coverage) obtained by fitting effective surface coverages according to the YNSN model, for wedges printed alone, for wedges printed in superposition with one solid ink and for wedges printed in superposition with two solid inks. The effective surface coverages, and therefore the dot gains, depend if a halftone wedge is printed alone, in superposition with one ink or in superposition with two inks. In Figure 2a, for ink-jet prints at 75 lpi, magenta halftones alone (m) have a nearly zero dot gain. Magenta halftones printed in superposition with solid cyan and solid yellow (m/cy) have the largest dot gain. However, as is shown in Figure 2b for thermal transfer prints at 75 lpi, ink spreading does not necessarily induce a larger dot gain when halftones are printed in superposition with one or two inks.

Since the surface coverages of the colorants for the dot-on-dot model are different from the ones for classical rotated dot screens, the ink spreading model for dot-on-dot printing is defined by its specific ink spreading equations. In dot-on-dot printing, the size relationship between surface coverages of cyan, magenta and yellow dots determines the contributing colorants. In the example of Figure 1, where the dot surface coverages are, from the smallest to the largest, cyan, magenta and yellow, i.e. $c <= m <= y$, ink spreading for cyan is determined only by the effective coverage of cyan superposed with the two other solid inks (black). The ink spreading of magenta depends on the ratio of the amount of magenta printed in superposition with the two other inks (black) and of the amount of magenta in superposition with yellow (red). The ink spreading of yellow depends on the ratio of the amount of yellow printed in superposition with the two other inks (black), printed in superposition with magenta (red) and printed on paper alone (yellow). Thus, under the condition: $c <= m <= y$, the ink spreading equations yielding the effective dot surface coverages of cyan, magenta and yellow are:

$$c' = f_{c/my}(c) \qquad \text{black colorant (superposed } c, m, y)$$

$$m' = f_{m/cy}(m)\ c'/\ m' + f_{m/y}(m)\ (m'-c')\ /\ m' \qquad \text{weights: surface ratios of black and red} \quad (4)$$

$$y' = f_{y/cm}(y)\ c'/\ y' + f_{y/m}(y)\ (m'-c')\ /\ y' + f_y(y)\ (y'-m')\ /\ y' \qquad \text{weights: surface ratios of black, red and yellow}$$

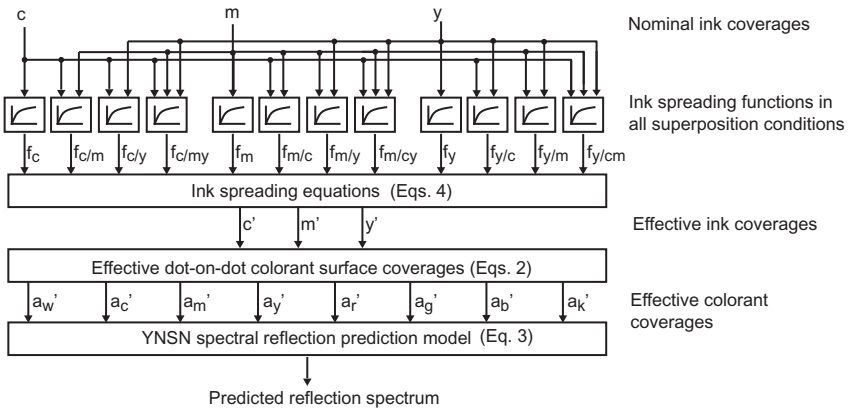

***Figure. 3**. Dot-on-dot spectral prediction model with dot gain and ink spreading in all superposition conditions*

Ink spreading equations similar to Eqs. (4) can be established for other size relationships of the ink dots (see columns of Table 2). For given nominal c, m, y surface coverages, only one of the columns is applicable for computing the corresponding effective surface coverages c', m', y' of cyan, magenta and yellow.

The system of equations (4) completed with the equations deduced from the columns of Table 2 can be solved iteratively: one starts by setting initial values of c', m' and y' equal to the respective nominal coverages c, m and y. After one iteration, one obtains new values for c', m' and y'. These new values are used for the next iteration. After a few iterations, typically 3 to 4 iterations, the system stabilizes and the obtained coverages c', m' and y' are the effective ink dot surface coverages (physical dot sizes) resulting from the combination of elementary ink surface coverages present in different superposition conditions. The effective colorant coverages a_w', a_c', .. a_k' are obtained from the effective coverages c', m' and y' of the inks according to equations (2) complemented with the equations deduced from Table 1**.**

Table 2. Ink spreading weights for each of the 6 possible dot surface relationships

Ink spreading functions	Weights of the ink spreading functions					
	$c\le m\le y$	$c\le y<m$	$m<c\le y$	$m\le y<c$	$y<c\le m$	$y<m<c$
cyan ink						
f_c	0	0	0	(c'-y')/c'	0	(c'-m')/c'
$f_{c/m}$	0	0	0	0	(c'-y')/c'	(m'-y')/c'
$f_{c/y}$	0	0	(c'–m')/c'	(y'-m')/c'	0	0
$f_{c/my}$	1	1	m'/c'	m'/c'	y'/c'	y'/c'
magenta ink						
f_m	0	(m'–y')/m'	0	0	(m'-c')/m'	0
$f_{m/c}$	0	0	0	0	(c'-y')/m'	(m'-y')/m'
$f_{m/y}$	(m'-c')/m'	(y'–c')/m'	0	0	0	0
$f_{m/cy}$	c'/m'	c'/m'	1	1	y'/m'	y'/m'
yellow ink						
f_y	(y'–m')/y'	0	(y'-c')/y'	0	0	0
$f_{y/c}$	0	0	(c'-m')/y'	(y'-m')/y'	0	0
$f_{y/m}$	(m'–c')/y'	(y'–c')/y'	0	0	0	0
$f_{y/cm}$	c'/y'	c'/y'	m'/y'	m'/y'	1	1

The complete model ink spreading in all superposition conditions is illustrated in Figure 3. By taking into account the effective ink dot surface coverages in all contributing superposition conditions, we obtain important improvements in spectral reflectance prediction accuracy. This is especially the case for ink-jet dot-on-dot prints where predictions in respect to single ink dot gain optimization (one reproduction curve per ink halftone) are improved by a factor of 2 to 3 (see Appendix).

Impact of the *n*-value

The n-value of the Yule-Nielsen modified spectral Neugebauer model depends on the ratio between lateral propagation of light within the paper bulk and the halftone screen period, on the multiple internal reflections between paper bulk and print-air interface as well as on possible non-uniformities in the dot thickness profiles. In order to better understand the signification of the n-value, let us plot the mean prediction error expressed in CIELAB−E_{94} values as a function of increasing n-values, for the considered printing technologies (ink-jet and thermal transfer).

Figures 4a and 4b show the mean prediction error (−E_{94}) as a function of the n-value, for the dot-on-dot Yule-Nielsen modified spectral Neugebauer model accounting for ink spreading in all superposition conditions.

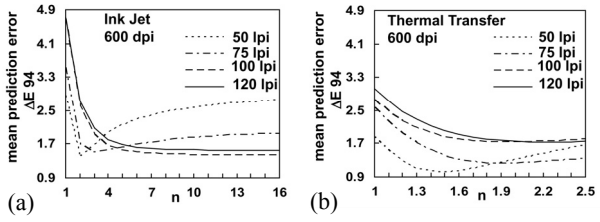

***Figure. 4**. Relationship between n-value and mean prediction error over 729 dot-on-dot print samples for (a) ink-jet prints at 50, 75, 100 and 120 lpi (b) thermal transfer prints at 50, 75, 100 and 120 lpi*

The mean prediction error is obtained by computing the $\Delta\Delta E_{94}$ color difference between predicted and measured spectra, for all 729 patches distributed uniformly over the full cyan, magenta and yellow color gamut. Figure 4 clearly shows that the optimal *n*-values increase with increasing screen frequency (lpi). However, at a high screen frequency (e.g. ink-jet at 100 lpi), the mean prediction error remains flat while increasing the *n*-value, meaning that a large range of *n*-values yield a similar prediction accuracy. One can also observe that for ink-jet, the optimal *n*-values are much smaller when taking into account ink spreading in all superposition conditions (see Appendix).

When creating the dot-on-dot YNSN model, the optimal *n*-value needs to be determined by relying on a small subset of print samples, e.g. the calibration samples needed for establishing the ink spreading functions (Figure 5). As a reference, we have also plotted the prediction accuracy as a function of *n*-value for the set of all test samples (729 samples).

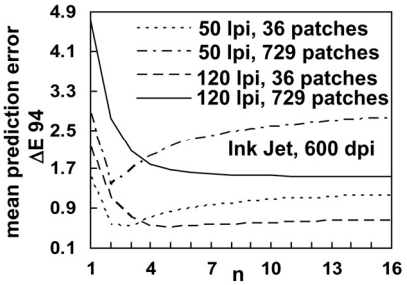

***Figure. 5**. Evolution of the mean prediction error in function of the n-value, in respect to learning sets comprising the samples used for establishing the ink spreading functions (ink-jet) and in respect to the full set of 729 dot-on-dot patches.*

Figure 5 shows that very similar optimal *n*-values are obtained in the case of ink-jet prints at 50lpi and 120 lpi for the calibration set comprising 36 samples and for the full set of 729 test samples. We can therefore compute a near optimal *n*-value by simply relying on the same set of measured samples as the one used for computing the ink spreading functions.

Application of the model

We carried out spectral predictions with the Yule-Nielsen modified Spectral Neugebauer model, on cyan, magenta and yellow dot-on-dot prints with screen dots oriented a 45° at various screen frequencies, both for ink-jet and for thermal transfer technologies. Printing devices are a thermal transfer wax printer (OKI DP-7000, 600 dpi, calendered paper) and an ink-jet printer (Canon PIXMA 4000 at 600dpi, coated paper) at screen frequencies of 50, 75, 100 and 120 lpi. The tables in the Appendix give the mean prediction errors in terms of ΔE_{94} values, the maximal prediction error and the number of patches having an error larger than $^{-}E_{94}$=3. For fitting the effective dot surface coverages, only 25%, 50% and 75% nominal coverages are used, yielding for ink spreading for all superposition conditions 3x12= 36 calibration patches. In addition, the spectral reflectances of the paper white and of patches of all solid inks and solid ink superpositions (colorants) are measured (8 patches). The model is tested on 729 patches, comprising all nominal coverage combinations at 0%, 13%, 25%, 38%, 50%, 63%, 75%, 88% and 100%. For comparison purposes, we also compute the accuracy of the spectral predictions with only one ink spreading function per ink [2] obtained by computing the effective surface coverages of single ink halftones printed on paper ("single ink dot gain only"). We also present the prediction accuracies for the same printing devices, same paper, same ink and same screen frequency, but for classical screens, mutually rotated by 30 degrees [15].

The prediction results clearly show that the *ink spreading* model improves the prediction accuracy. In respect to the *thermal transfer* technology (Appendix), the ink spreading model improves the prediction of reflection spectra by up to 50%, similar to the improvement brought to classical mutually rotated screens. Classical mutually rotated screens offer a slightly better prediction accuracy (lower average ΔE_{94} color difference). However, at 120 lpi, when the dots become unstable due to the high screen frequency, dot-on-dot provides a higher prediction accuracy, presumably because of more stable screen dots.

In respect to the *ink-jet* technology (Appendix), accounting for ink spreading in all superposition conditions improves the spectral reflectance prediction accuracy by a factor of 2 to 3, both for dot-on-dot screens and for classical mutually rotated screens. In terms of absolute prediction accuracy, since classical rotated screens are less sensitive to misregistration errors than dot-on-dot halftones [6], they provide approximately a 50% higher prediction accuracy.

Conclusions

We have developed a new approach for modeling *ink spreading*, a phenomenon which occurs when printing an ink halftone superposed with paper, with one or with several solid inks. In the present contribution, we develop specific ink spreading equations for dot-on-dot printing. Ink spreading functions map nominal to effective surface coverages of an ink halftone for single ink halftones printed alone, ink halftones superposed with a second solid ink and ink halftones superposed with two solid inks. When predicting the reflection spectrum of a dot-on-dot halftone patch, its known nominal surface coverage values are converted into effective surface coverage values by weighting the contributions from different ink spreading functions (reproduction curves) according to the corresponding ratios of colorant surface coverages.

For calibrating the functions mapping nominal to effective surface coverages in the different superposition conditions, effective surface coverage values are fitted by minimizing the sum of square differences between measured and predicted reflection density spectra. In the case of three inks (cyan, magenta and yellow), the calibration set comprises 44 samples. The same halftone print samples used to calibrate the ink spreading model can also be used for computing for given printing conditions (print technology, screen frequency, inks, paper) the near optimal *n*-value of the Yule-Nielsen modified spectral Neugebauer model.

When applying the Yule-Nielsen modified spectral Neugebauer model for predicting the reflection spectra of dot-on-dot halftone patches, accounting for ink spreading in all ink superposition conditions improves the spectral reflectance predictions for thermal transfer by a factor up to 1.5 and for ink-jet by a factor up to 3.

Since dot-on-dot printing is more sensitive to misregistration errors than classical mutually rotated screens, the prediction accuracy for dot-on-dot printing remains below the one for classical mutually rotated screens. We conjecture that the present dot-on-dot spectral prediction model may also provide a feedback about the registration accuracy of a dot-on-dot printing device.

References

1. D.R. Wyble, R.S. Berns , A Critical Review of Spectral Models Applied to Binary Color Printing, J. Color Res. Appl., Vol. 25, No. 1, 4-19, (2000).
2. R. Balasubramanian, Optimization of the spectral Neugebauer model for printer characterization, J. Electronic Imaging, Vol. 8, No. 2, 156-166, (1999).
3. J.A.C. Yule , W.J. Nielsen, The penetration of light into paper and its effect on halftone reproductions, Proc. TAGA, Vol. 3, 65-76, (1951)
4. J.A.S Viggiano, Modeling the Color of Multi-Colored Halftones, Proc. TAGA, 44-62, (1990).
5. Amidror, R.D. Hersch, V. Ostromoukhov, Spectral analysis and minimization of moiré patterns in color separation, J. Electronic Imaging, Vol. 3, 295-317, (1994).
6. B. Oztan, G. Sharma, R.P. Loce, Quantitative Evaluation of Misregistration Induced Color Shifts in Color Halftones, Proc. SPIE Vol. 5667, 501-512, (2005).
7. R. Balasubramanian, A printer model for dot-on-dot halftone screens, Proc. SPIE Vol. 2413, 356-364, (1995).
8. H.R. Kang, Color Technology for Electronic Imaging Devices, SPIE Optical Engineering Press, (1997).
9. H.E.J. Neugebauer, Die theoretischen Grundlagen des Mehrfarbendrucks. Zeitschrift fuer wissenschaftliche Photographie, Vol. 36, 36-73, (1937), reprinted in Neugebauer Seminar on Color Reproduction, SPIE Vol 1184,194-202 (1989).
10. H.R. Kang, Applications of color mixing models to electronic printing, J. of Electronic Imaging, Vol. 3, No. 3, 276-287, (1994)
11. K. Iino, R.S. Berns, Building color management modules using linear optimization I. Desktop, J. of Imaging Sci. and Techno., Vol. 42, No. 1, 79-94, (1998).
12. K. Iino, R.S. Berns, Building color management modules using linear optimization II, Prepress system for offset printing, J. of Imaging Sci. and Techno., Vol. 42, No. 2, 99-114, (1998).
13. U. Agar and J. P. Allebach, "An Iterative Cellular YNSN Method for Color Printer Calibration," Proc. 6th IS&T/SID Color Imaging Conference, pp. 197-200, (1998).
14. P. Emmel, R.D. Hersch, Modeling ink spreading for color prediction, J. of Imaging Sci. and Techno., Vol. 46, No. 3, 237-246, (2002).
15. R.D. Hersch, F. Crété, Improving the Yule-Nielsen modified spectral Neugebauer model by dot surface coverages depending on the ink superposition conditions, SPIE Vol. 5667, 434-445, (2005).
16. S. Zuffi, R. Schettini, An innovative method for spectral-based printer characterization, SPIE Vol. 4663, 1-7, (2002).
17. M. Xia, E. Saber, G. Sharma, M. Tekalp, End to end color printer calibration by total least squares regression, IEEE Trans. On Image Processing, Vol. 8, No. 5, 700-716, (1999).
18. G. Rogers, A Generalized Clapper-Yule Model of Halftone Reflectance, J. Color Res. Appl., Vol. 25, No. 6, 402-407 (2000).
19. M. Hebert, R.D. Hersch, Classical Print Reflection Models, a Radiometric Approach, J. of Imaging Sci. and Techno., Vol. 48, No. 4, 363-374, (2004).

Appendix: Prediction accuracies for thermal transfer prints and for ink jet prints

729 test samples for thermal transfer prints and for ink jet prints	lpi	Dot on Dot Halftone Screen				Classical Halftone Screen			
		n	Max $\Delta-E_{94}$	Mean $-E_{94}$	# samples $-E_{94}$>3	n	Max $-E_{94}$	Mean $-\Delta E_{94}$	# samples $-E_{94}$>3
Thermal Transfer prints (OKI DP-7000)									
Single ink dot-gain only	**50**	1.4	5.16	1.19	1	1.6	3.99	1.27	10
Ink spreading in all superposition conditions		1.5	3.31	1.02	2	1.3	3.09	0.95	2
Single ink dot-gain only	**75**	1.6	5.03	1.90	78	1.9	4.67	1.59	30
Ink spreading in all superposition conditions		2.0	4.09	1.23	11	1.4	3.98	1.22	23
Single ink dot-gain only	**100**	1.5	5.26	1.96	90	4.1	4.57	1.97	92
Ink spreading in all superposition conditions		2.0	5.15	1.72	91	1.9	4.30	1.49	25
Single ink dot-gain only	**120**	1.6	5.13	1.90	74	2.9	6.23	2.52	243
Ink spreading in all superposition conditions		2.2	5.95	1.73	96	1.5	5.93	2.07	147
Ink-jet prints (Canon Pixma 4000)									
Single ink dot-gain only	**50**	3.7	12.83	3.52	362	2.1	7.07	2.13	150
Ink spreading in all superposition conditions		1.9	3.91	1.38	31	1.9	3.50	1.19	3
Single ink dot-gain only	**75**	11.8	12.44	3.60	394	3.6	9.36	2.87	283
Ink spreading in all superposition conditions		3.0	3.99	1.49	53	3.1	2.37	1.00	0
Single ink dot-gain only	**100**	29.0	15.34	5.06	565	18.0	8.65	3.18	346
Ink spreading in all superposition conditions		12.6	4.01	1.44	43	6.9	2.58	0.98	0
Single ink dot-gain only	**120**	32.0	13.51	4.53	513	25.0	8.81	3.32	383
Ink spreading in all superposition conditions		14.5	4.35	1.55	68	11.0	2.90	0.87	0